JLAB-THY-08-864

An estimate of the prehadron production time

Alberto Accardi[a,b]
[a] *Hampton University, Hampton, VA, 23668, USA*
[b] *Jefferson Lab, Newport News, VA 23606, USA*

A semi-quantitative estimate of the prehadron production time based on recent preliminary HERMES data on hadron transverse momentum broadening in nuclear DIS is presented. The obtained production time can well explain the data except for their dependence on the photon virtuality, which remains a challenge to current theoretical models. A few mechanisms that may contribute to its explanation are suggested, along with possible experimental tests. The average time scale at HERMES is found to be of the order of 4-5 fm, comparable to heavy nuclei radii, so that by suitable kinematic cuts it will be possible to study both the case in which hadronization starts inside and the case in which it starts outside the nucleus. A comparison with recent CLAS preliminary data, which qualitatively but not quantitatively agree with HERMES, is performed.

I. INTRODUCTION

Nuclear modifications of hadron production in high-energy collisions have been observed in both Deep Inelastic lepton-nucleus Scattering (nDIS) [1] and in heavy ion collisions [2–5]. One typically observes: (i) a suppression of hadron multiplicities, called hadron quenching or jet quenching; (ii) hadron transverse momentum (p_T) broadening; (iii) the related modification of the hadron p_T-spectrum also known as Cronin effect. The nuclear modifications can be attributed to the interactions of the scattered partons and of the hadrons formed in their fragmentation with the surrounding medium. Experimentally, partonic in-medium interactions can be isolated by studying Drell-Yan (DY) lepton pair production in hadron-nucleus collisions. In nDIS and hadron-nucleus collisions, the medium is the nuclear target itself, also called "cold nuclear matter". In nucleus-nucleus collisions, the fragmenting parton must also traverse the hot and dense medium created in the collisions, be it a hadron gas at low energy, or a Quark-Gluon Plasma (QGP) at high energy. This medium is also called "hot nuclear matter".

A precise knowledge of parton propagation and hadronization mechanisms obtained from nDIS and DY data is essential for testing and calibrating our theoretical tools, and to determine the properties of the QGP produced at the Relativistic Heavy Ion Collider. Conversely, a well known nuclear medium like a target nucleus allows testing the hadronization mechanism and color confinement dynamics in nDIS. Knowledge of partonic in-medium propagation gained from nDIS, can be used in DY scatterings to factor out parton energy loss and measure the nuclear modifications of parton distributions in the initial state [6]. Finally, hadron quenching is an important source of systematic uncertainty in neutrino oscillation experiments such as MINOS, which use nuclear targets and need to reconstruct the event's kinematic from the hadronic final state [7, 8].

Understanding and modeling nuclear modifications of hadron production requires knowledge of the space-time evolution of the hadronization process [9]. However, hadronization is a non perturbative process, and its theoretical understanding is still in its infancy: one has to resort to phenomenological models to describe its space-time evolution [10–16]. Nonetheless, a few features can be expected on general grounds. A parton created in a high-energy collision can travel as a free particle only for a limited time because of color confinement: it has to dress-up in a color-field of loosely bound partons, which eventually will evolve into the observed hadron wave function. While the naked, asymptotically free, parton has a negligible inelastic cross section with the surrounding medium constituents, the dressed parton is likely to develop an inelastic cross section of the order of the hadronic one. Hence, the dressed parton will be subject to nuclear absorption in a similar way a fully formed hadron is. For this reason, it is usually called "prehadron", and denoted by h_*. The prehadron may for some time be in a colored state, h_*^c, because color neutrality is only required for the final state hadron. However, it is likely to neutralize its color before hadron formation, and the colorless prehadron is denoted h_*^0. We can therefore identify 3 relevant time scales, see Fig. 1: (1) the "prehadron production time" or "quark lifetime" t_p, at which the dressed quark develops a sizable inelastic cross section, (2) the "color neutralization time" t_{cn}, at which gluon bremsstrahlung stops, and (3) the "hadron formation time" t_h, at which the final hadron is formed.

For practical applications, hadronization is generally pictured as a 2 step process in which the prehadron pro-

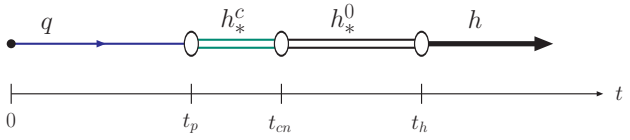

FIG. 1: Sketch of the time evolution of the hadronization process with definition of the relevant time scales. A quark q created at time 0 in a hard collision turns into a colored prehadron h_*^c, which subsequently neutralizes its color, h_*^0, and collapses on the wave function of the observed hadron h.

duction time and color neutralization time are identified, $t_p = t_{cn}$. This is a somewhat crude approximation of the more complex process sketched above, but is adequate to the present status of the theoretical and experimental investigation and will be used in this paper.

In summary, the key quantity we need to investigate in order to understand this complex dynamics is the hadronization time scale, t_p. It is the most general information about the space-time evolution of the hadronization process which can be extracted from experimental data. It is the purpose of this paper to provide a semi-quantitative and model independent estimate of the prehadron production time from recent preliminary data on the p_T-broadening taken by the HERMES experiment in lepton-nucleus scatterings at the HERA accelerator [17–19]. These data show rich features in terms of their dependence on the kinematic variables, which are confirmed by preliminary data taken by the CLAS experiment at Jefferson Lab [20–22], and are not always simple to interpret theoretically. I will show to what extent a consistent picture of the space-time evolution of hadronization can be inferred from these data, and how they are beginning to expose the limits of current theoretical modeling of this process.

II. PRODUCTION TIME SCALING

Hadron quenching in nDIS is studied in terms of the multiplicity ratio

$$R_M^h(z,\nu,p_t^2,Q^2) = \frac{\left.\frac{N_h(z,\nu,p_t^2,Q^2)}{N_e(\nu,Q^2)}\right|_A}{\left.\frac{N_h(z,\nu,p_t^2,Q^2)}{N_e(\nu,Q^2)}\right|_D}, \qquad (1)$$

where N_h is the yield of semi-inclusive hadrons in a given kinematic bin, and N_e the yield of inclusive scattered leptons in the same (ν,Q^2)-bin. The kinematic variables z, ν, p_t^2, Q^2 are the usual DIS invariants, namely, the hadron fractional energy, the virtual photon energy, the hadron transverse momentum and the lepton 4-momentum transfer squared.

In Ref. [23] it is conjectured that R_M should not depend on z and ν separately but should depend on a combination of them:

$$R_M = R_M\big[\tau(z,\nu)\big] \ , \qquad (2)$$

where the scaling variable τ is defined as

$$\tau = C\, z^\lambda (1-z)\nu \ . \qquad (3)$$

The scaling exponent λ can be obtained by a best fit analysis of data or theoretical computations. Obviously, the proportionality constant C cannot be determined by the fit. A possible scaling of R_M with Q^2 is not considered because of its model dependence, and because of the mild dependence of HERMES R_M data on Q^2. As discussed below, the proposed functional form of τ, Eq. (3), is flexible enough to encompass both absorption models, which assume short production times and in-medium hadronization, and energy loss models, which assume long lived quarks with $\langle t_p\rangle \gg R_A$, where R_A is the nuclear radius. The 2 classes of models are distinguished by the value of the scaling exponent: a positive $\lambda \gtrsim\!\!\!\not\; 0$ is characteristic of absorption models, while a negative $\lambda \lesssim 0$ is characteristic of energy loss models. Thus, the exponent λ extracted from experimental data can identify the leading mechanism for hadron suppression in nDIS, and distinguish short from long hadronization time scales.

The scaling of R_M is quite natural in the context of hadron absorption models [10–15]. Indeed, prehadron absorption depends on the in-medium prehadron path length, which depends on the prehadron production time $\langle t_p\rangle$, as long as $\langle t_p\rangle \lesssim R_A$. In the Lund string model [24] hadronization is modeled by the breaking of the color string stretching from the struck parton to the target remnant. The production time is

$$\langle t_p\rangle = f(z)(1-z)\frac{zE_q}{\kappa_{\rm str}} \qquad (4)$$

where E_q is the struck quark energy, and $\kappa_{\rm str}$ the string tension. At leading order (LO) in the Strong coupling constant α_s, the partonic subprocess is $\gamma^* + q \to q$ and one obtains

$$E_q = \nu \ . \qquad (5)$$

The factor zE_q can be understood as a Lorentz boost factor. The $(1-z)$ factor is due to energy conservation: a high-z hadron carries away an energy zE_q; the string remainder has a small energy $\epsilon = (1-z)E_q$ and cannot stretch farther than $L = \epsilon/\kappa_{str}$. Thus the string breaking must occur on a time scale proportional to $1-z$. The function $f(z)$ is a small deformation of $\langle t_p\rangle$, which can be computed analytically in the standard Lund model [10, 13]. The main features of the estimate (4) are dictated by kinematics and 4-momentum conservation, hence are of general nature. Indeed they can be obtained also by perturbative considerations based on the uncertainty principle, similarly to what is discussed in Ref. [25], or in the perturbative hadronization model of Ref. [11]. The production time (4) is well described by the proposed scaling variable τ with $\lambda > 0$. E.g., in the Lund model $\lambda \approx 0.7$ [23]. In energy loss models [26–28], which assume $\langle t_p\rangle \gg R_A$, the scaling is less obvious and holds only approximately on a theoretical ground. When performing the scaling analysis of the full energy loss models, one finds in general $\lambda \lesssim 0$ [23].

The central result of the analysis of HERMES data at $E_{\rm lab} = 27$ GeV performed in Ref. [23] is that pion data clearly exhibit

$$\lambda \approx 0.5 \gtrsim\!\!\!\not\; 0 \ . \qquad (6)$$

As discussed, this is a signal of in-medium prehadron formation, with production times $\langle t_p\rangle = O(R_A)$. Therefore,

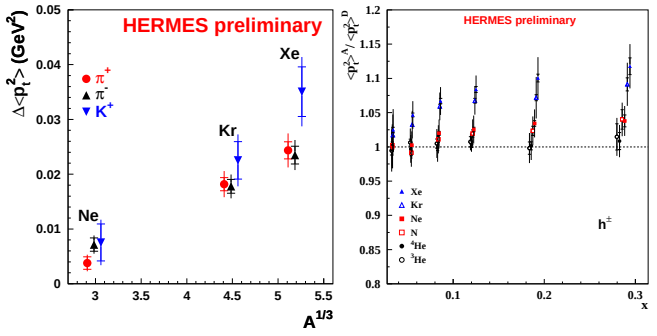

FIG. 2: Left: p_t-broadening at HERMES for different hadron types produced from several nuclear targets as a function of the atomic number A (from Refs. [17, 18]). Right: Ratio $\langle p_T^2\rangle_A/\langle p_T^2\rangle_D$ as a function of x_B (from Ref. [19]). The inner error bars represent the statistical error and the outer ones the quadratic sum of the statistical and systematic uncertainties.

the scaling variable τ can be identified with the average production time:

$$\langle t_p\rangle \equiv \tau \ . \tag{7}$$

The proportionality constant C in Eq. (3), hence the magnitude of the production time, will be estimated in Section III. A similar analysis has been attempted in Ref. [1], but arbitrarily fixing $\lambda = 0.35$. The resulting $R_M(\tau)$ shows a rough scaling, with the 2 lowest-z data point in each data set deviating from the scaling curve and aligning in the vertical direction. This breaking of the scaling behavior is more probably due to the particular choice of λ, rather than to rescattering effects as argued by the authors.

III. p_T-BROADENING AND PREHADRON FORMATION

The scaling analysis just described gives only indirect evidence for a short production time $\langle t_p\rangle$, and cannot measure its absolute scale. An observable which is more directly related to the prehadron production time, and allows an estimate of the coefficient C in Eq. (3), is the hadron's transverse momentum broadening in DIS on a nuclear target compared to a proton or deuteron target [11, 29],

$$\Delta\langle p_T^2\rangle = \langle p_T^2\rangle_A - \langle p_T^2\rangle_D \ . \tag{8}$$

When a hadron is observed in the final state, neither the quark nor the prehadron from which it originates could have had inelastic scatterings. Since the prehadron-nucleon elastic cross section is very small compared to the quark cross section, the hadron's p_T-broadening originates dominantly during parton propagation. As shown in [30, 31], the quark's momentum broadening $\Delta\langle p_T^2\rangle$ is proportional to the quark path-length in the nucleus. If the prehadron production time has the form (3) as argued in the last section, and as long as the prehadron is

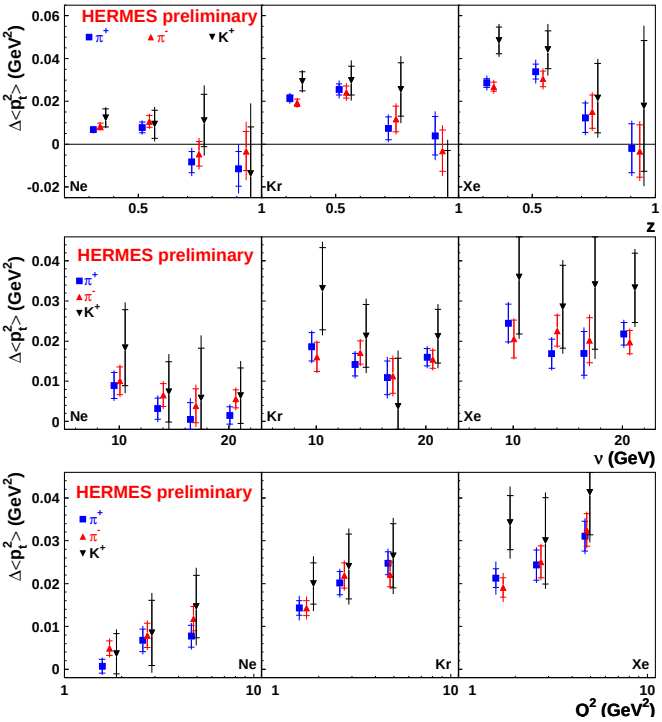

FIG. 3: As Figure 2, but for the p_t-broadening as a function of z (upper panel), ν (middle panel), and Q^2 (lower panel). Plots taken from Refs. [17, 18].

formed inside the nucleus, we obtain

$$\Delta\langle p_T^2\rangle \propto \langle t_p\rangle \propto z^{0.5}(1-z)\nu \ , \tag{9}$$

where the exponent 0.5 is determined by the scaling analysis discussed in Section II. Then, a decrease of Δp_T^2 with increasing z or decreasing ν would be a clear signal of in-medium prehadron formation: indeed, if the quark were traveling through the whole nucleus before prehadron formation, Δp_T^2 would only depend on the nucleus size and not on z or ν. In addition to the dependence of $\Delta\langle p_T^2\rangle$ on z and ν, which primarily stems from energy conservation and the Lorentz boost of the hadron, Ref. [11] argues that

$$\Delta\langle p_T^2\rangle \propto \frac{1}{Q^2} \ . \tag{10}$$

The physics behind this proposed behavior is that a quark which is struck by a photon of large virtuality radiates more intensely than for a lower virtuality: as a consequence, it will be able to only travel a shorter way before hadronization, hence it will experience less p_T-broadening. A related observable is the Cronin effect, which is likewise expected to decrease with increasing z or decreasing ν, and possibly with increasing Q^2 [11].

The HERMES preliminary data on the p_T-broadening, reproduced in Figs. 2 and 3 for the reader's convenience, show a linear increase with $A^{1/3}$, and a clear decrease of $\Delta\langle p_T^2\rangle$ at large z consistent with Eq. (9) and HERMES data on the Cronin effect [1]. However, HERMES data

	$\langle Q^2\rangle$ [GeV^2]	$\langle\nu\rangle$ [GeV]	$\langle z\rangle$	$\frac{\langle Q^2\rangle}{2m_N\langle\nu\rangle}$	$\langle t_p\rangle$ [fm]
$\langle\Delta p_{Th}^2\rangle$ vs A					
Ne (2.3 fm)	2.4	13.7	0.42	0.09	4.2
Kr (3.7 fm)	2.4	13.9	0.41	0.09	4.2
Xe (4.3 fm)	2.4	14.0	0.41	0.09	4.3
$\langle\Delta p_{Th}^2\rangle$ vs z	2.4	14.6	0.30	0.09	4.5
	2.4	13.3	0.53	0.10	3.7
	2.3	12.6	0.74	0.10	2.3
	2.2	10.8	0.92	0.11	0.7
$\langle\Delta p_{Th}^2\rangle$ vs ν	2.1	8.1	0.48	0.14	2.4
	2.5	12.0	0.42	0.11	3.7
	2.6	15.0	0.40	0.10	4.6
	2.4	18.6	0.36	0.07	5.8
$\langle\Delta p_{Th}^2\rangle$ vs Q^2	1.4	14.0	0.41	0.06	4.2
	2.4	14.1	0.41	0.10	4.2
	4.5	14.5	0.39	0.16	4.3

TABLE I: Average HERMES kinematics for the p_T-broadening results [17, 18]. In parenthesis, beside the target nucleus symbol is the average in-medium path length of the hadronizing system $\langle L_A\rangle \approx (3/4)R_A$, with $R_A = (1.12\text{ fm})A^{1/3}$. The production time is computed according to Eq. (12). The average $\langle x_B\rangle$ is very well approximated by $\langle Q^2\rangle/(m_N\langle\nu\rangle)$ [32].

also show a clearly increasing $\Delta\langle p_T^2\rangle$ with $Q^2 = 2-10$ GeV^2, at variance with the Q^2 dependence of the prehadron production time (10) obtained in Ref. [11], and with string models in general. They also show an increase of $\langle p_T^2\rangle|A/\langle p_T^2\rangle|D$ with x_B tending to saturate at $x_B \gtrsim 0.2$ [19]. The flat, or even slightly decreasing dependence of $\Delta\langle p_T^2\rangle$ on ν is also, at first sight, not easily interpreted in the context of Eq. (9) and the simple hadronization picture used so far.

For a more quantitative interpretation of the data we have first to specify the average kinematics in each bin, see Table I and Ref. [18]. Indeed, different observables and different experimental bins may be related to different prehadron production times. To this purpose, let us consider the A and z distributions:

- The scaling of $\Delta\langle p_T^2\rangle \propto A^{1/3}$ up to the Xe nucleus indicates that the quark path length is larger than the average in-medium path length $\langle L_{\rm Xe}\rangle$ of the hadronizing system in the Xe nucleon at $\langle z\rangle \approx 0.4$, $\langle\nu\rangle \approx 14$ GeV, so that the prehadron is always formed on the surface or outside the nucleus.

- The above kinematics is close to that of the first 2 z-bins at $z = 0.30$ and 0.53. Hence we may assume that also in these 2 bins the prehadron is formed on the surface or outside the nucleus. However, given the decrease of $\Delta\langle p_T^2\rangle$ with z as $z \gtrsim 0.5$, the prehadron must soon enter the nucleus at larger z. Hence, the production time at $z \approx 0.4$ fm cannot be much larger than $\langle L_{\rm Xe}\rangle$.

These 2 remarks allow setting the scale for the production time in Eq. (3):

$$C \approx \frac{\langle L_{\rm Xe}\rangle}{\bar z^{\lambda}(1-\bar z)\bar\nu} \approx 0.8\frac{\rm fm}{\rm GeV} \qquad (11)$$

with $\bar z = 0.4$ and $\bar\nu = 14$ GeV. The average in-medium path-length of the hadronizing system can be approximated as $\langle L_{\rm Xe}\rangle \approx (3/4)R_A$ with $R_A = (1.12\text{ fm})A^{1/3}$, as if nucleons were uniformly distributed in the nucleus. The resulting production time,

$$\langle t_p\rangle \approx 0.8\, z^{0.5}(1-z)\,\nu\text{ fm/GeV}\ , \qquad (12)$$

with ν measured in GeV, is plotted in Fig. 4. In principle, C should be allowed to depend on Q^2 and x_B, but one can neglect it in first approximation at least for the discussion of the A-, z-, where $\langle Q^2\rangle$ and $\langle x_B\rangle$ are rather constant. With Eq. (12), we can compute the production times for each experimental bin, see Table I.

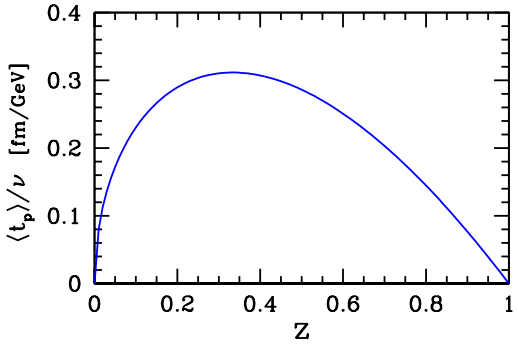

FIG. 4: z dependence of the prehadron production time $\langle t_p\rangle/\nu \equiv \tau\nu$ extracted from HERMES data.

The ν-distribution is also consistent with this estimate: given the production times in Table I, it is not too surprising that the ν-dependence is basically flat, because the prehadron is formed on average on the surface or outside all the studied nuclei. Three effects can contribute to tilt the curve and producing the slightly decreasing data: (i) a possible dependence of the prehadron cross section with ν, as it happens for the hadron cross section; (ii) medium modifications of the DGLAP parton shower [33–36], which can modify the linear dependence of $\Delta\langle p_T^2\rangle$ on the energy loss ΔE found in [30], and implicit in Eq. (9); (iii) the correlation between the p_T-broadening and the average Bjorken variable, $\langle x_B\rangle$, whose origin will be discussed in detail in the next Section, and which may in fact be the dominant effect.

IV. p_T-BROADENING VS. Q^2 AND x_B

We are now in the position to address the intriguing Q^2 distribution. The linear increase of $\Delta\langle p_T^2\rangle$ with Q^2 is in sharp contrast with the inverse power dependence obtained in the color dipole model, see Eq. (10). On the other hand also a flat Q^2, as would be obtained in most

string-based models, seems at variance with these data. To my knowledge, no model predicts a substantial rise of $\langle t_p \rangle$ with virtuality: how can we explain these data? From the production times shown in Table I, we can see that the prehadron is always formed on the surface or outside the nucleus, so that the observed Q^2-dependence must predominantly have a partonic origin. It cannot simply come from multiple parton elastic scatterings, because it would be in first order proportional to the in-medium parton path-length, which is basically fixed. The following 3 mechanisms may contribute to explain these data:

1. *Medium-enhanced DGLAP evolution.* The DGLAP evolution in the kinematics under consideration happens entirely inside the nucleus, because the prehadron is produced at its surface. The scale Q_0^2 at which hadronization takes place is not expected to strongly depend on the presence of a medium [44]. Therefore, in the large-Q^2 bins, a longer and medium-enhanced DGLAP evolution [33–36] would imply a larger p_T-broadening than at low Q^2 . How strong this effect is, and whether it can lead to a linear increase of the p_T-broadening with Q^2 remains to be seen. This mechanism can be investigated with a $\nu > \nu_{\rm min}$ cut in the experimental data: as $\nu_{\rm min}$ is increased, the DGLAP evolution would increasingly happen outside the nucleus, and the slope in Q^2 should become smaller and smaller.

2. *Next-to-leading order processes.* The basic hard partonic process considered so far is the leading order in α_s quark elastic scattering $\gamma^* + q \to q$. It is the dominant process in the valence region at large x_B. As x_B decreases, however, the gluon distribution in the nucleon quickly rises, so that the photon-gluon fusion process $\gamma^* + g \to q + \bar{q}$, which is a next-to-leading order (NLO) process, becomes non negligible. In this case the photon energy ν is shared by the quark and the antiquark, so that $E_q < \nu$, therefore reducing the quark lifetime and its p_T-broadening compared to the LO case where $E_q = \nu$. As can be seen from Table I, the average $\langle x_B \rangle$ spanned in the Q^2 distribution lies in the transition region between sea partons and valence quark dominance. Hence, the competition between LO and NLO process might alter the naive picture of p_T-broadening adopted so far, and lead to its increase with Q^2. This mechanism may also be at work in ν-distributions, although with smaller effects because of the more limited range spanned by $\langle x_B \rangle$, and contribute to tilt their slope downwards. Note that if this mechanism is indeed at work, the estimate of C presented in Eq. (11) only gives a lower limit on the hadron production time. Experimentally, this mechanism can be tested by measuring Q^2-distributions with suitable cuts on x_B. The slope in Q^2 should become flat at very small or large $\langle x_B \rangle$, see the discussion below.

3. *Colored prehadrons with short formation times.* A more radical possibility is that at these values of $\langle \nu \rangle$, the quark does not propagate freely for a long time; instead, shortly after the hard interaction, it turns into a colored prehadron h_*^c which can loose energy by gluon bremsstrahlung, thereby broadening its transverse momentum. The prehadron may have an inelastic cross section $\propto 1/Q^2$, growing in time to the full hadronic one. If the time evolution is slow enough, at low Q^2 the prehadron would be subject to more nuclear absorption than at large Q^2, explaining the linear rise of $\Delta\langle p_T^2 \rangle$ with Q^2 [45]. An extreme version of this mechanism would involve

$$\begin{aligned} \langle t_p \rangle &\approx 0 \\ \langle t_{cn} \rangle &\approx 0.8\, z^{0.5}(1-z)\, \nu \text{ fm/GeV} . \end{aligned} \tag{13}$$

   Note that this scenario does not contradict the dipole model prediction that $\langle t_p \rangle \propto 1/Q^2$, but would require the prehadron to propagate as a colored state for a time of the order of the nuclear radius. An experimental investigation of this scenario needs very large ν, outside the reach of the HERMES experiment but attainable at the Electron-Ion Collider (EIC) [37, 38], in order to significantly boost $\langle t_p \rangle$ and allow the quark to propagate as a free particle inside the nucleus.

In order to study the physics behind the experimental correlation of $\Delta\langle p_T^2 \rangle$ with x_B and Q^2, one needs to simultaneously address Q^2-distributions binned in x_B and x_B-distributions binned in Q^2. In this way, one can factor out the trivial kinematic correlation $\nu = Q^2/(2m_N x_B)$ which affects the production time. For example, if $\langle t_p \rangle \propto \nu/\kappa$ with κ fixed, as in the Lund string model, for the LO $\gamma^* + q \to q$ scattering we should expect

$$\begin{aligned} Q^{-2}\Delta\langle p_T^2 \rangle_{x_B\text{-bins}} &\approx \text{const.} \\ x_B \Delta\langle p_T^2 \rangle_{Q^2\text{-bins}} &\approx \text{const.} \end{aligned} \tag{14}$$

The deviation from this *combined* scaling is going to expose the underlying dynamics, see Table II: if mechanism number 2 is dominant, we would observe $Q^{-2}\Delta\langle p_T^2 \rangle_{x_B}$ constant in Q^2 but $x_B\Delta\langle p_T^2 \rangle_{Q^2}$ increasing with x_B; mechanisms number 1 or 3 would produce an increasing $Q^{-2}\Delta\langle p_T^2 \rangle_{x_B}$ but a constant $x_B\Delta\langle p_T^2 \rangle_{Q^2}$. In the color dipole model [11], $t_p \propto \nu/Q^2 \propto 1/x_B$ hence $Q^{-2}\Delta\langle p_T^2 \rangle_{x_B}$ would be decreasing and $x_B\Delta\langle p_T^2 \rangle_{Q^2}$ constant.

It is also important to extend as much as possible the range in x_B over which the p_T-broadening is measured: at small $x_B \lesssim 0.01$ the NLO photon-gluon fusion is the dominant partonic process, while at $x_B \gtrsim 0.3 - 0.4$ the photon dominantly scatters at LO valence quarks. Hence, with mechanism number 2, one may expect $\Delta\langle p_T^2 \rangle$ to flat in Q^2 in these 2 regions.

model		$Q^{-2}\Delta\langle p_T^2\rangle_{x_B}$ vs. Q^2	$x_B\Delta\langle p_T^2\rangle_{Q^2}$ vs. x_B
$t_p \propto \nu/\kappa$	LO	$\leftrightarrow$	$\leftrightarrow$
	mDGLAP (1)	$\uparrow$	$\leftrightarrow$
	NLO vs. LO (2)	$\leftrightarrow$	$\uparrow$
	colored h_c^* (3)	$\uparrow$	$\leftrightarrow$
$t_p \propto \nu/Q^2$	color dipole [11]	$\downarrow$	$\leftrightarrow$

TABLE II: Expected results of the scaling analysis of the p_T-broadening for the models and mechanisms discussed in this paper. The numbers in parenthesis refer to the mechanisms listed in Section IV. The up and down pointing arrows indicate increasing or decreasing p_T-broadening, the double horizontal arrow an approximately constant behavior.

V. COMPARISON TO CLAS PRELIMINARY DATA

A last question needs to be addressed: how do the HERMES data and these scenarios compare to preliminary CLAS data [20–22] on the p_T-broadening and Cronin effect?

At CLAS, the higher beam luminosity allows multi-dimensional binning which is only partly accessible at HERMES. The kinematics is a bit different due to the lower beam energy, $E_{\rm beam} = 5$ GeV compared to 27 GeV. The main difference is that $\langle\nu\rangle = 2-5$ GeV is much smaller than at HERMES, therefore prehadron production should typically happen on shorter time scales, mainly inside the nucleus according to the estimate (9). Note also that $Q^2 = 1-4$ GeV^2, and that, typically, $\langle x_B\rangle_{\rm CLAS} > \langle x_B\rangle_{\rm HERMES}$. The main features of CLAS data on C, Fe, and Pb targets are the following:

- The p_T-broadening is linear in $A^{1/3}$ at low A, but tends to saturate for large nuclei. The flattening is confirmed by the lack of increase in the Cronin effect from the Fe target to the Pb target. This shows the prehadron being formed on a time scale $t_p \gtrsim (4/3)R_{\rm Fe} = 4.3$ fm, smaller than at HERMES.
- The p_T-broadening is rising and then saturating with ν. The saturation appears at $\nu \gtrsim 4$ GeV, where the HERMES p_T is also approximately flat.
- The Cronin effect decreases with z as it happens at HERMES.
- The Cronin effect markedly increases as x_B increases from 0.1 to 0.5. This confirms the x_B dependence of HERMES p_T-broadening.

All these features corroborate the discussed HERMES data. However, the production time I have estimated is about a factor 5 smaller than the production time extracted in Ref. [29] from CLAS ν-distributions using the color dipole formalism [31]. On the other hand, based on this paper's analysis, and taking into account the uncertainty in the estimate of $\langle L_A\rangle$, HERMES data can only support up to a doubling of t_p, which would otherwise become incompatible with the large-z decrease of the p_T-broadening. The HERMES and CLAS data sets may be qualitatively reconciled by taking into account the observed increase of the p_T-broadening with $\langle x_B\rangle$ discussed in the previous Section. Indeed, $\langle x_B\rangle_{\rm CLAS} > \langle x_B\rangle_{\rm HERMES}$, which implies a larger p_T-broadening at CLAS.

The origin of the discrepancy between the production times extracted from HERMES and CLAS data on the p_T-broadening remains to be clarified. On the theoretical side, the two discussed methods to determine the production time should be applied to both data sets, in order to check their consistency and further explore the issue. On the experimental side, it is very important to establish and study the correlation of $\Delta\langle p_T^2\rangle$ with x_B and Q^2, as emphasized in the previous section.

VI. CONCLUSIONS

In this paper, I attempted a semi-quantitative estimate of the prehadron production time, based on recent preliminary HERMES data on hadron p_T-broadening in nuclear DIS, see Eq. (12). The obtained production time can well explain the dependence of the p_T-broadening on A, z and ν. Its linear increase with Q^2 remains a challenge to current theoretical models, and I proposed a few mechanisms that may contribute to its explanation, also suggesting how to experimentally validate them. Furthermore, I discussed how the preliminary CLAS data qualitatively support the features observed at HERMES.

With the obtained estimate of t_p, the prehadrons at HERMES are typically formed around the nuclear surface or slightly outside, while at CLAS they are typically formed inside the target. However, a quantitative analysis indicate that $t_p|_{\rm HERMES} \approx 0.2 t_p|_{\rm CLAS}$. The observed x_B dependence of the p_T-broadening can at least in part reconcile the 2 data sets, as well as explain the Q^2 dependence of the data. It also points at a non-negligible role of NLO processes in the hadronization process.

The measurement of hadron p_T-broadening, and the related Cronin effect, are beginning to test the limits of current theory models on the space-time evolution of hadronization, which are based on LO γ^*-quark scattering, followed by color neutralization of the quark and hadron formation. The main theoretical challenges raised by these data are, in my opinion,

- the inclusion of NLO processes in the modeling of hadron quenching.
- the implementation at LO, and subsequently at NLO, of alternative models of energy loss, like a medium-modified DGLAP evolution;
- testing of alternative space-time pictures beyond the 2 time scale models currently accepted; for example, the role of a colored prehadron should be explored.

On the experimental side, the proposed physics mechanisms can be verified by measuring the p_T-broadening and the Cronin effect with suitable kinematic cuts. In particular,

- the role of parton energy loss can be highlighted by large-ν/small-z cuts, such that the parton lifetime exceeds the nuclear size;
- in-medium hadronization can be selected by small-ν/large-z cuts;
- the x_B dependence of $\Delta\langle p_T^2\rangle$, the Cronin effect, and the multiplicity ratio needs to be better studied over a large interval of x_B, including small $x_B \lesssim 0.01$ and large $x_B \gtrsim 0.4$; additionally, dihadron correlations and the hadron multiplicity per event as a function of x_B can more directly reveal the role of NLO processes, in which 2 partons can be produced at the hard scattering;
- the combined analysis of p_T-broadening's x_B-distributions binned in Q^2 and of Q^2-distributions binned in x_B is likely to usefully expose the underlying dynamics.

Because of the available ν range, the HERMES experiment and the future Electron-Ion Collider are best suited to study the role of parton energy loss and propagation in cold nuclear matter. At CLAS, in-medium hadronization is likely to be dominant and can be studied in detail thanks to its high-statistics data, which allow multidimensional binning and the study of one kinematic variable at a time.

Acknowledgments

I would like to thank E. Aschenauer, W. Brooks, J. Morfín for interesting and informative discussions. I am grateful to P. di Nezza and Y. Van Haarlem for additionally and carefully reading the manuscript. This work has been supported by the DOE contract No. DE-AC05-06OR23177, under which Jefferson Science Associates, LLC operates Jefferson Lab, and NSF award No. 0653508.

[1] A. Airapetian *et al.* [HERMES], Nucl. Phys. B **780**, 1 (2007).
[2] I. Arsene *et al.* [BRAHMS], Nucl. Phys. A **757** (2005) 1.
[3] B. B. Back *et al.*, Nucl. Phys. A **757**, 28 (2005).
[4] J. Adams *et al.* [STAR], Nucl. Phys. A **757**, 102 (2005).
[5] K. Adcox *et al.* [PHENIX], Nucl. Phys. A **757**, 184 (2005)
[6] G. T. Garvey and J. C. Peng, Phys. Rev. Lett. **90** (2003) 092302.
[7] P. Adamson *et al.* [MINOS], arXiv:0806.2237 [hep-ex].
[8] S. Dytman, H. Gallagher and M. Kordosky, arXiv:0806.2119 [hep-ex].
[9] A. Accardi, Eur. Phys. J. C **49** (2007) 347.
[10] A. Bialas and M. Gyulassy, Nucl. Phys. B **291** (1987) 793.
[11] B. Z. Kopeliovich, J. Nemchik, E. Predazzi and A. Hayashigaki, Nucl. Phys. A **740** (2004) 211.
[12] A. Accardi, V. Muccifora and H. J. Pirner, Nucl. Phys. A **720** (2003) 131.
[13] A. Accardi, D. Grunewald, V. Muccifora and H. J. Pirner, Nucl. Phys. A **761** (2005) 67.
[14] T. Falter, W. Cassing, K. Gallmeister and U. Mosel, Phys. Rev. C **70** (2004) 054609.
[15] K. Gallmeister and T. Falter, Phys. Lett. B **630** (2005) 40.
[16] K. Gallmeister and U. Mosel, Nucl. Phys. A **801**, 68 (2008).
[17] Y. Van Haarlem, A. Jgoun and P. di Nezza [HERMES], arXiv:0704.3712 [hep-ex].
[18] Y. Van Haarlem, "The HERMES recoil photon-detector and nuclear p(t)-broadening at HERMES,", Ph.D. thesis, DESY-THESIS-2007-033, Sep 2007. Thesis and preliminary plots available at [42].
[19] A. Jgoun, preliminary analysis of HERMES data available at [42].
[20] K. Hafidi [CLAS], AIP Conf. Proc. **870** (2006) 669.
[21] W. K. Brooks [CLAS], talk presented at [43]
[22] K. Hicks [CLAS], talk presented at [43]
[23] A. Accardi, Phys. Lett. B **649** (2007) 384.
[24] B. Andersson *et al.*, Phys. Rept. **97** (1983) 31.
[25] A. Adil and I. Vitev, Phys. Lett. B **649** (2007) 139.
[26] E. Wang and X. N. Wang, Phys. Rev. Lett. **89** (2002) 162301.
[27] F. Arleo, Eur. Phys. J. C **30** (2003) 213.
[28] A. Accardi, Acta Phys. Hung. A **27**, 189 (2006).
[29] B. Z. Kopeliovich, J. Nemchik and I. Schmidt, Nucl. Phys. A **782** (2007) 224.
[30] R. Baier, Y. L. Dokshitzer, A. H. Mueller, S. Peigne and D. Schiff, Nucl. Phys. B **484** (1997) 265.
[31] M. B. Johnson, B. Z. Kopeliovich and A. V. Tarasov, Phys. Rev. C **63** (2001) 035203.
[32] Y. Van Haarlem, private communication.
[33] F. A. Ceccopieri and L. Trentadue, Phys. Lett. B **660** (2008) 43.
[34] S. Domdey, G. Ingelman, H. J. Pirner, J. Rathsman, J. Stachel and K. Zapp, arXiv:0802.3282 [hep-ph].
[35] N. Borghini and U. A. Wiedemann, arXiv:hep-ph/0506218.
[36] N. Armesto, L. Cunqueiro, C. A. Salgado and W. C. Xiang, JHEP **0802** (2008) 048.
[37] A. Deshpande, R. Milner, R. Venugopalan and W. Vogelsang, Ann. Rev. Nucl. Part. Sci. **55** (2005) 165.
[38] EIC homepage, `http://web.mit.edu/eicc/`
[39] F. E. Close, R. L. Jaffe, R. G. Roberts and G. G. Ross, Phys. Rev. D **31** (1985) 1004.
[40] J. Dias de Deus, Phys. Lett. B **166**, 98 (1986).
[41] A. Accardi, talk at the *Workshop on "Electromagnetic*

interactions on nucleons and nuclei", Santorini (Greece), October 2003.

[42] HERMES documents repository, available at `http://www-hermes.desy.de/notes/`.

[43] Workshop on "Parton fragmentation processes: in the vacuum and in the medium", ECT*, Trento (ITA), 25-29 February 2008. Talks available at `arleo.web.cern.ch/arleo/ff_vacuum_medium_ect08/`.

[44] The partial deconfinement of bound nucleons in a nucleus [39] may induce an A-dependence of Q_0 and modify hadron fragmentation [12, 40]. However, such an effect is unfavored by the measured Q^2 dependence of R_M, which is opposite than what is expected in the partial deconfinement mechanism [41].

[45] A similar space-time evolution of hadronization has been implemented for leading prehadrons in the GiBUU absorption model of Refs. [14, 16], which however assumes $t_p = t_{cn} = 0$ for leading (but colorless) prehadrons, and does not address radiative energy loss. It would be interesting to phenomenologically include both a colored and a colorless prehadron in this model to test the proposed scenario.